J. Fluid Mech. (1983), *vol.* 132, *pp.* 395–406
Printed in Great Britain

A porous-wavemaker theory

By ALLEN T. CHWANG
Institute of Hydraulic Research, The University of Iowa, Iowa City, Iowa 52242

(Received 7 September 1982 and in revised form 3 March 1983)

A porous-wavemaker theory is developed to analyse small-amplitude surface waves on water of finite depth, produced by horizontal oscillations of a porous vertical plate. Analytical solutions in closed forms are obtained for the surface-wave profile, the hydrodynamic-pressure distribution and the total force on the wavemaker. The influence of the wave-effect parameter C and the porous-effect parameter G, both being dimensionless, on the surface waves and on the hydrodynamic pressures is discussed in detail.

1. Introduction

Surface waves forced by a wavemaker were treated by the classical wavemaker theory developed by Havelock (1929), Biesel & Suquet (1951) and Ursell, Dean & Yu (1960). In this classical wavemaker theory, the wavemaker was represented by a vertical impermeable plate which oscillates horizontally with a small displacement, and the amplitude of the forced surface waves was assumed to be small.

For small-amplitude surface waves produced by a moving vertical plate starting from rest, Kennard (1949) presented a linear wave theory based on the Fourier integral method. Adopting Kennard's solution, Madsen (1970) analysed the particular problem of a sinusoidally moving piston-type wavemaker starting from rest. Recently, Chwang (1983) presented a nonlinear theory to analyse the impulsive motion of a vertical plate. Using the method of small-time expansions, Chwang was able to obtain analytical solutions up to and including the third-order velocity potential. The free-surface profile of the fluid was also determined analytically.

The effect of finite inclination angle of a wavemaker on the surface waves was studied by Raichlen & Lee (1978). They investigated numerically and experimentally the linear surface waves produced by an inclined-plate wave generator which is hinged at the bottom. They found that, for a given stroke and depth-to-wavelength ratio, very small waves were produced; for other wave periods for the same conditions significantly larger waves were generated.

The influence of leakage around the wavemaker on the wave amplitude was analysed by Madsen (1970). He found that the leakage effect was large in reducing the wave amplitude. The purpose of the present paper is to analyse the porous effect of a wavemaker on the free-surface waves. This porous-wavemaker theory may have important applications in the study of surface waves in reservoirs or lakes caused by landslides during earthquakes. Water waves are generated by landslides which may occur either vertically, inclined at an angle, or horizontally over a portion of their travel. Noda (1970) has modelled a vertical landslide by a two-dimensional box which falls to the bottom at the end of a semi-infinite channel. He also modelled a horizontal landslide by a two-dimensional wall which moves into the fluid domain. In both of his models, the box and the wall are impermeable. When the bulk mass in a landslide

consists of rocks and soils, a porous box or wall would be more appropriate. Thus the results of the present paper could lead to a better analysis of landslide-generated surface waves. Another possible application of the present analysis is in situations where efficiency of generation of waves is of main interest, with the wavemaker being subjected to some form of structural constraint on the maximum allowable force. A porous wavemaker may be helpful in reducing the total load which is accompanied by a reduction of wave amplitude as the porous-effect parameter G (defined in (23b)) increases.

The general problem of surface waves on water of finite depth, produced by horizontal oscillations of a porous vertical plate, is formulated in §2. The boundary condition on the surface of the porous wavemaker is derived based on Taylor's (1956) assumption that the velocity perpendicular to the porous plate is linearly proportional to the difference in pressure between the two sides of the wavemaker. The hydrodynamic-pressure distribution and the total force on the wavemaker, and the surface-wave profile have been obtained analytically in §3. Finally, the numerical results are presented and discussed in §4.

2. Formulation of the problem

Let us consider a porous piston-type wavemaker. The mean position of the wavemaker is at the $x = 0$ plane (see figure 1). It oscillates horizontally along the x-axis with a displacement s_0:

$$s_0 = d\,\mathrm{e}^{\mathrm{i}\omega t} \quad (d \ll h), \tag{1}$$

where ω is the circular frequency, d the maximum amplitude of oscillation, which is assumed to be small in comparison with the undisturbed fluid depth h. The y-axis points vertically upwards, with the plane $y = 0$ being the bottom. The horizontal velocity and acceleration of the wavemaker are

$$u_0 = \mathrm{i}\omega d\,\mathrm{e}^{\mathrm{i}\omega t}, \quad a_0 = -\omega^2 d\,\mathrm{e}^{\mathrm{i}\omega t} \tag{2}$$

respectively. Owing to the oscillation of the wavemaker, small-amplitude surface waves are produced which propagate away from the wavemaker. The disturbed free surface is at $y = h + \eta(x, t)$, where η is much smaller than h.

We shall assume the fluid to be incompressible and inviscid, and its motion irrotational. Therefore the velocity potential $\Phi(x, y, t)$ satisfies the Laplace equation

$$\nabla^2\Phi = 0. \tag{3}$$

The linearized kinematic condition and dynamic condition on the free surface are

$$\Phi_y = \eta_t \quad (y = h), \tag{4}$$

$$\Phi_t + g\eta = 0 \quad (y = h) \tag{5}$$

respectively, where Φ_y denotes $\partial\Phi/\partial y$ etc. Combining (4) and (5), we have the linearized free-surface condition for Φ:

$$\Phi_{tt} + g\Phi_y = 0 \quad (y = h). \tag{6}$$

At the bottom $y = 0$, the vertical velocity of the fluid must vanish. Hence

$$\Phi_y = 0 \quad (y = 0). \tag{7}$$

In the linear theory, the hydrodynamic pressure $P(x, y, t)$ is related to the velocity

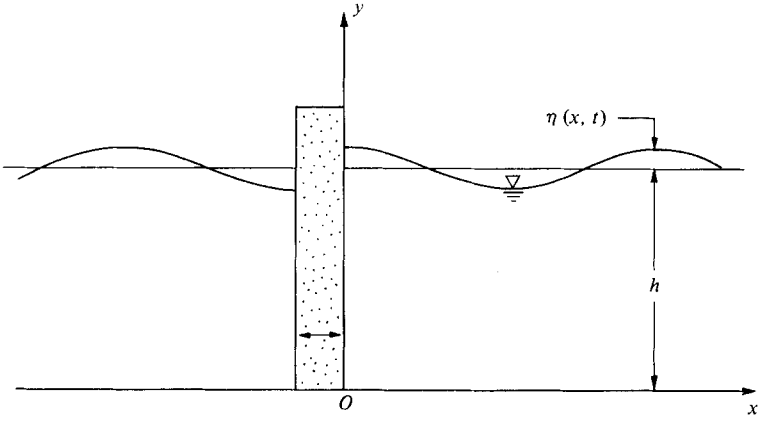

FIGURE 1. Schematic diagram of a porous wavemaker.

potential Φ by the Bernoulli equation as

$$P = -\rho\Phi_t, \tag{8}$$

where ρ is the constant density of the fluid. Owing to the linearity of the problem and the antisymmetry of the wavemaker motion, the hydrodynamic pressure on the positive side of the wavemaker surface, $P^+(y,t)$, is related to that on the negative side of the plate, $P^-(y,t)$, by

$$P(0,y,t) = P^+(y,t) = -P^-(y,t). \tag{9}$$

We shall assume that the porous wavemaker is made of material with very fine pores. The normal velocity of the fluid passing through the porous plate is thus linearly proportional to the pressure difference between the two sides of the wavemaker (Taylor 1956):

$$W(y,t) = \frac{b}{\mu}(P^+ - P^-) = \frac{2b}{\mu}P(0,y,t), \tag{10}$$

where μ is the dynamic viscosity and b is a coefficient which has the dimension of a length.

In the present paper, we shall analyse the waves on the positive side of the wavemaker ($x > 0$). Waves generated to the left of the wavemaker can be analysed similarly. The boundary condition on the wavemaker surface is

$$\Phi_x = u_0 - W \quad (x = 0), \tag{11}$$

where u_0 and W are given by (2) and (10) respectively. It should be noted that, if the porous flow through the wavemaker is significant, Taylor's assumption (10) and the boundary condition (11) may not be accurate enough. Hence, we should confine our analysis to porous wavemakers with fine pores.

3. Pressure force and surface-wave profile

Based on the periodic motion of the wavemaker, we assume that the velocity potential, the hydrodynamic pressure and the normal velocity in the porous plate are all periodic functions in t and have a time factor $\exp(\mathrm{i}\omega t)$:

$$\Phi = \phi(x,y)\,\mathrm{e}^{\mathrm{i}\omega t}, \quad P = p(x,y)\,\mathrm{e}^{\mathrm{i}\omega t}, \quad W = w(y)\,\mathrm{e}^{\mathrm{i}\omega t}. \tag{12}$$

By (3) and (12), $\phi(x, y)$ also satisfies the Laplace equation

$$\phi_{xx}+\phi_{yy}=0. \tag{13}$$

The solution of (13), satisfying the boundary conditions (6) and (7), which corresponds to an outgoing wave in the region $x > 0$, can be obtained by the method of separation of variables as

$$\phi = A_0 \cosh k_0 y\, \mathrm{e}^{-\mathrm{i}k_0 x}+\sum_{n=1}^{\infty} A_n \cos k_n y\, \mathrm{e}^{-k_n x}, \tag{14}$$

where k_0 satisfies the relation

$$1-Ck_0 h \tanh k_0 h=0, \tag{15a}$$

k_n are the roots of

$$1+Ck_n h \tan k_n h=0 \quad (n=1,2,3,\ldots), \tag{15b}$$

and C is a wave-effect parameter (Chwang 1981) defined by

$$C=\frac{g}{\omega^2 h}. \tag{15c}$$

A_0 and A_n $(n = 1, 2, 3, \ldots)$ in (14) are arbitrary constants. We note that (15a, c) give the usual dispersion relation for surface waves in a fluid of constant depth h:

$$\omega^2 = gk_0 \tanh k_0 h. \tag{16}$$

By (2), (11), (12) and (14), we have

$$\mathrm{i}\omega d-w(y) = -\mathrm{i}k_0 A_0 \cosh k_0 y-\sum_{n=1}^{\infty} k_n A_n \cos k_n y. \tag{17}$$

Since the eigenfunctions $\cosh k_0 y$ and $\cos k_n y$ $(n = 1, 2, 3, \ldots)$ are orthogonal over the interval from $y = 0$ to $y = h$, we obtain the constants A_0 and A_n as

$$A_0 = -\frac{2\omega d P_0}{k_0^2 h(1+CP_0^2)}-\frac{2\mathrm{i}}{k_0 h(1+CP_0^2)}\int_0^h w(y)\cosh k_0 y\,\mathrm{d}y, \tag{18a}$$

$$A_n = -\frac{2\mathrm{i}\omega d P_n}{k_n^2 h(1-CP_n^2)}+\frac{2}{k_n h(1-CP_n^2)}\int_0^h w(y)\cos k_n y\,\mathrm{d}y, \tag{18b}$$

where

$$P_0 = \sinh k_0 h, \quad P_n = \sin k_n h \quad (n=1,2,3,\ldots). \tag{19}$$

On the other hand, (10) together with (8), (12) and (14) give

$$\mu w(y) = -2\mathrm{i}\omega b\rho(A_0 \cosh k_0 y+\sum_{n=1}^{\infty} A_n \cos k_n y). \tag{20}$$

Again, based on the orthogonality of the eigenfunctions, we have from (20)

$$A_0 = \frac{\mathrm{i}\mu}{\omega b\rho h(1+CP_0^2)}\int_0^h w(y)\cosh k_0 y\,\mathrm{d}y, \tag{21a}$$

$$A_n = \frac{\mathrm{i}\mu}{\omega b\rho h(1-CP_n^2)}\int_0^h w(y)\cos k_n y\,\mathrm{d}y. \tag{21b}$$

Equating (18) to (21), we obtain

$$\int_0^h w(y)\cosh k_0 y\,\mathrm{d}y = \frac{2\mathrm{i}\omega^2 bd\rho P_0}{\mu k_0^2(1+G_0)}, \tag{22a}$$

$$\int_0^h w(y)\cos k_n y\,\mathrm{d}y = \frac{2\mathrm{i}\omega^2 bd\rho P_n}{\mu k_n^2(G_n-\mathrm{i})} \quad (n=1,2,3,\ldots), \tag{22b}$$

where

$$G_0 = \frac{k_1}{k_0} G, \quad G_n = \frac{k_1}{k_n} G \quad (n = 1, 2, 3, \ldots), \tag{23a}$$

$$G = \frac{2\rho\omega b}{\mu k_1}. \tag{23b}$$

Therefore the coefficients A_0 and A_n can be expressed explicitly as

$$A_0 = -\frac{2\omega d P_0}{k_0^2 h (1 + CP_0^2)(1 + G_0)}, \tag{24a}$$

$$A_n = -\frac{2\omega d P_n}{k_n^2 h (1 - CP_n^2)(G_n - \mathrm{i})} \quad (n = 1, 2, 3, \ldots). \tag{24b}$$

The hydrodynamic-pressure distribution on the wavemaker surface, normalized with respect to $\rho h(-\omega^2 d)$, is (taking the real part only)

$$\frac{P(0, y, t)}{-\rho\omega^2 dh} = C_\mathrm{p} \cos\omega t + C_\mathrm{q} \sin\omega t, \tag{25a}$$

where the in-phase (with respect to the horizontal displacement of the wavemaker) pressure coefficient C_p is given by (8), (12), (14) and (24) as

$$C_\mathrm{p} = \sum_{n=1}^{\infty} \frac{2P_n \cos k_n y}{k_n^2 h^2 (1 - CP_n^2)(1 + G_n^2)}, \tag{25b}$$

and the out-of-phase pressure coefficient C_q is given by

$$C_\mathrm{q} = \frac{2P_0 \cosh k_0 y}{k_0^2 h^2 (1 + CP_0^2)(1 + G_0)} + \sum_{n=1}^{\infty} \frac{2P_n \cos k_n y}{k_n^2 h^2 (1 - CP_n^2)(G_n + G_n^{-1})}. \tag{25c}$$

Alternatively, the dimensionless pressure distribution on the wavemaker surface may be expressed as

$$C_\mathrm{p} \cos\omega t + C_\mathrm{q} \sin\omega t = D_\mathrm{p} \cos(\omega t - \theta_\mathrm{p}), \tag{26a}$$

where

$$D_\mathrm{p} = (C_\mathrm{p}^2 + C_\mathrm{q}^2)^{\frac{1}{2}}, \quad \theta_\mathrm{p} = \tan^{-1} \frac{C_\mathrm{q}}{C_\mathrm{p}}. \tag{26b}$$

The total hydrodynamic pressure force on the wavemaker, normalized with respect to $\rho h^2(-\omega^2 d)$, is obtained by integrating (25) with respect to y from $y = 0$ to $y = h$,

$$C_\mathrm{F} \cos\omega t + C_\mathrm{L} \sin\omega t = D_\mathrm{F} \cos(\omega t - \theta_\mathrm{F}), \tag{27a}$$

where

$$D_\mathrm{F} = (C_\mathrm{F}^2 + C_\mathrm{L}^2)^{\frac{1}{2}}, \quad \theta_\mathrm{F} = \tan^{-1} \frac{C_\mathrm{L}}{C_\mathrm{F}}, \tag{27b}$$

$$C_\mathrm{F} = h^{-1} \int_0^h C_\mathrm{p}(y)\, \mathrm{d}y = \sum_{n=1}^{\infty} \frac{2P_n^2}{k_n^3 h^3 (1 - CP_n^2)(1 + G_n^2)}, \tag{27c}$$

$$C_\mathrm{L} = \frac{2P_0^2}{k_0^3 h^3 (1 + CP_0^2)(1 + G_0)} + \sum_{n=1}^{\infty} \frac{2P_n^2}{k_n^3 h^3 (1 - CP_n^2)(G_n + G_n^{-1})}. \tag{27d}$$

The free-surface elevation measured from the undisturbed level at $y = h$, $\eta(x, t)$, is obtained from (5), (12), (14) and (24) by taking the real part only. Thus

$$\frac{\eta}{d} = E_0 \sin(k_0 x - \omega t) + \sum_{n=1}^{\infty} (E_n \cos\omega t + F_n \sin\omega t)\, \mathrm{e}^{-k_n x}, \tag{28a}$$

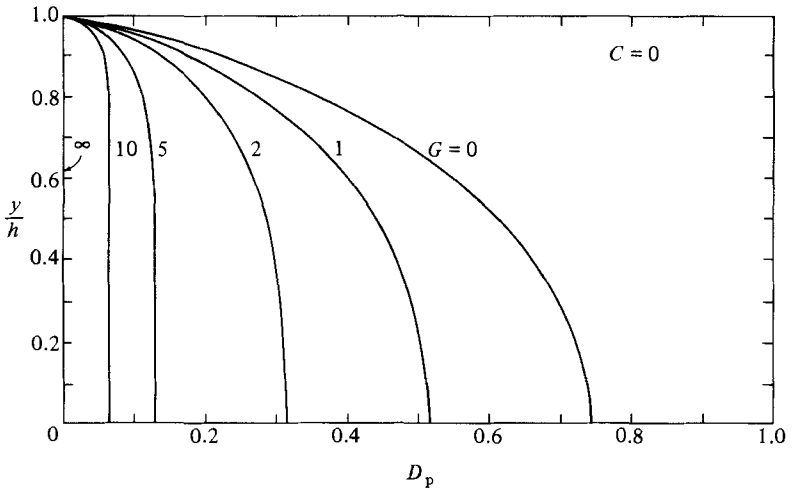

FIGURE 2. The hydrodynamic pressure distribution on the wavemaker surface for various values of G at $C = 0$.

where

$$E_0 = \frac{2P_0^2}{k_0 h(1+CP_0^2)(1+G_0)}, \tag{28b}$$

$$E_n = \frac{2P_n^2}{k_n h(1-CP_n^2)(1+G_n^2)} \quad (n = 1,2,3,\ldots), \tag{28c}$$

$$F_n = \frac{2P_n^2}{k_n h(1-CP_n^2)(G_n+G_n^{-1})} \quad (n = 1,2,3,\ldots). \tag{28d}$$

The first term in (28a) represents a progressive wave propagating away from the wavemaker along the positive x-direction. The second term in (28a) corresponds to the sum of non-propagating waves whose amplitudes decay exponentially as x increases.

4. Results and discussion

The dimensionless pressure coefficient D_p defined by (26) and (25) is plotted in figure 2 versus the vertical distance y/h at $C = 0$ for several different values of G. The wave-effect parameter C defined by (15c) is a direct measure of the ratio of the gravity effect to the inertial effect due to oscillation of the wavemaker. A small value of C means that the gravity effect is negligible. $C = 0$ indicates no surface waves. On the other hand, for large values of C, the surface gravity waves become important. The parameter G defined in (23) may be viewed as a Reynolds number for the flow passing through the fine pores of the porous wavemaker. It is also a measure of the porous effect. $G = 0$ means that the wavemaker is impermeable. On the other hand, as G approaches infinity, the wavemaker is completely permeable to fluid; that is, there would be no wavemaker at all. In figure 3, the phase angle θ_p for the pressure distribution on the wavemaker surface, defined in (26), is plotted versus the vertical distance y/h at $C = 0$ for several different values of G. We note from figures 2 and 3 that both D_p and θ_p increase as the height y/h decreases for fixed values of G. They reach maximum values at the bottom $y = 0$. At a fixed height of y/h, D_p decreases while θ_p increases as G increases. At $G = 0$, the wavemaker becomes impermeable,

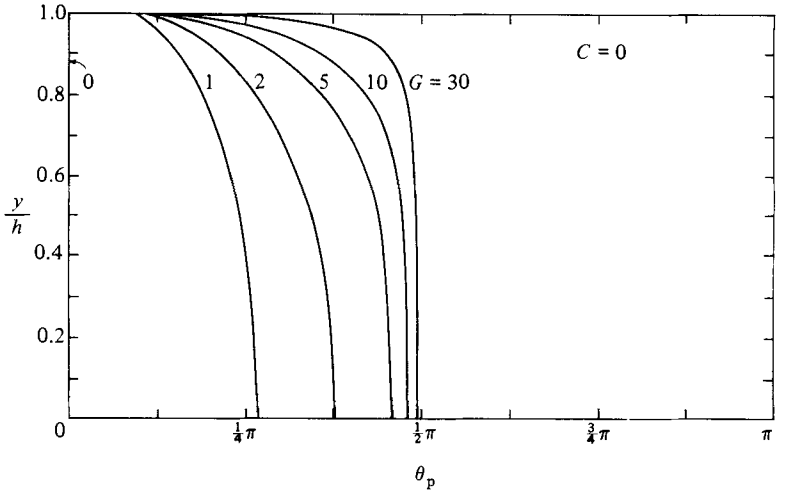

FIGURE 3. The phase angle of pressure distribution for various values of G at $C = 0$.

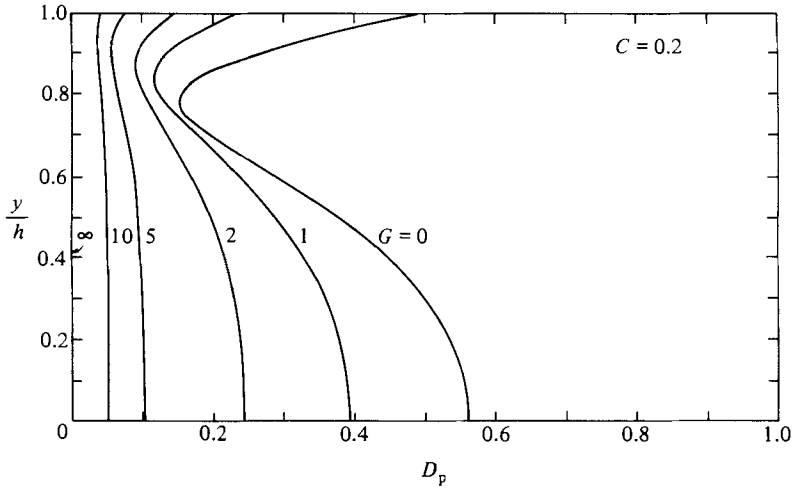

FIGURE 4. The hydrodynamic-pressure distribution on the wavemaker surface for various values of G at $C = 0.2$.

θ_p reduces to zero. It means that the hydrodynamic pressure is in phase with the displacement of the wavemaker. Also, D_p tends to the maximum distribution at $G = 0$, which agrees exactly with that for a vertical plate (Chwang 1978) and in a fluid of constant density (Chwang 1981). As G approaches infinity, the wavemaker becomes completely permeable to fluid, or it disappears functionally such that D_p reduces to zero as shown in figure 2.

The surface-wave effect on the hydrodynamic pressure distribution is shown in figures 4 and 5, in which the dimensionless pressure coefficient D_p and the phase angle θ_p are plotted respectively versus the vertical distance y/h at $C = 0.2$ for various values of the porous-effect parameter G. We note from these two figures that D_p and θ_p are no longer monotonic functions of y/h for fixed values of G. D_p decreases initially as y/h increases from zero, similar to the case of $C = 0$. It then increases as y/h further increases close to the free surface because of the presence of surface waves there. We

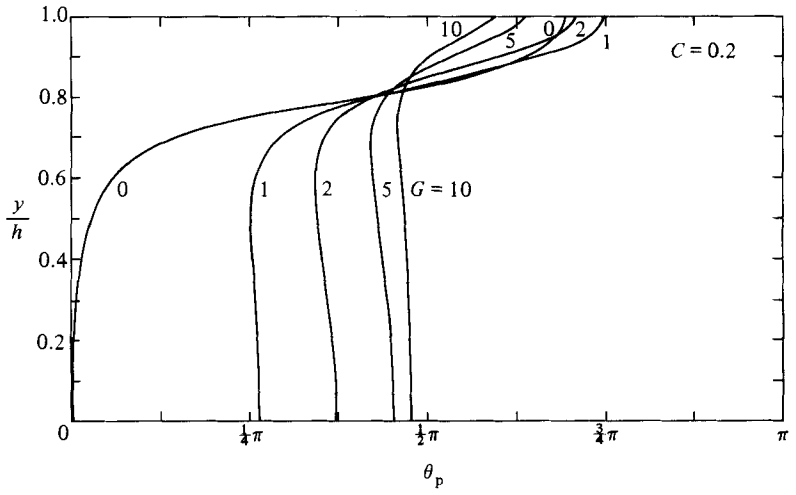

FIGURE 5. The phase angle of pressure distribution for various values of G at $C = 0.2$.

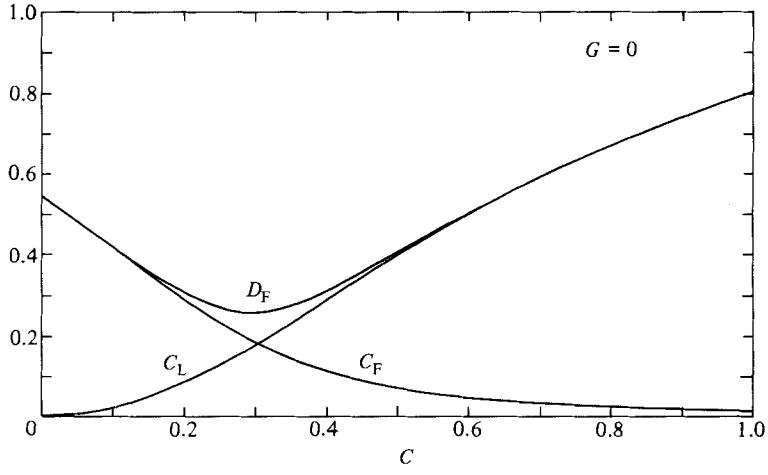

FIGURE 6. The in-phase force coefficient C_F, the out-of-phase force coefficient C_L, and the total force coefficient D_F versus the wave-effect parameter C at $G = 0$.

should note that the free surface is no longer at $y = h$ but $h+\eta(x,t)$. Hence the pressure coefficient D_p does not vanish at $y = h$ – it takes a value corresponding to the hydrostatic pressure due to the wave height η. For an impermeable wavemaker ($G = 0$) the value of D_p at the bottom $y = 0$ is smaller than that for $C = 0$, and the phase angle θ_p is very close to zero near the bottom at $C = 0.2$. θ_p increases with an increase in height. As y/h approaches unity, θ_p exceeds $\frac{1}{2}\pi$ owing to the presence of surface waves.

For an impermeable wavemaker ($G = 0$), the in-phase force coefficient C_F, the out-of-phase force coefficient C_L, and the total force coefficient D_F are shown in figure 6 as functions of the wave-effect parameter C as computed from equations (27c, d, b) respectively. We note from figure 6 that, at $C = 0$, C_L vanishes while C_F has its maximum value of 0.543, which is precisely the value given by Westergaard (1933) and by Chwang (1981) when the surface waves are absent. As the value of C increases,

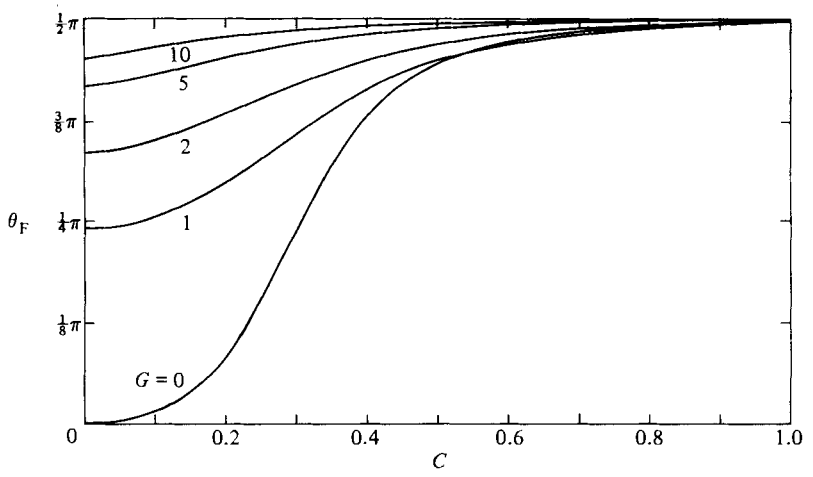

FIGURE 7. The phase angle of total force versus the wave-effect parameter C for various values of G.

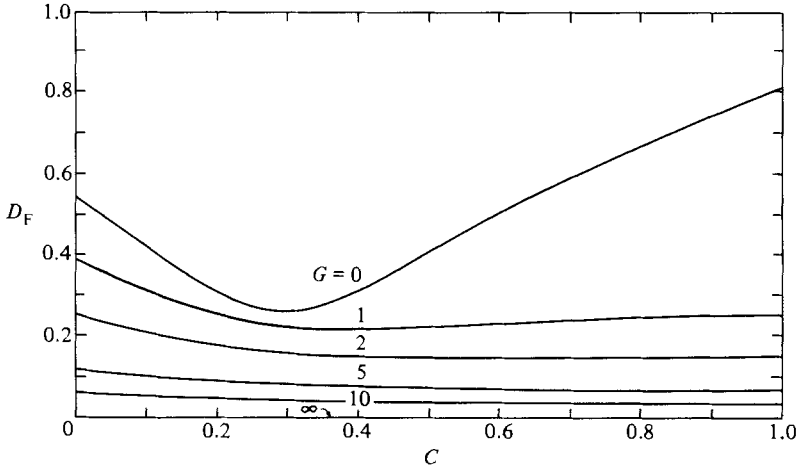

FIGURE 8. The total force coefficient versus the wave-effect parameter C at several different values of the porous-effect parameter G.

C_F decreases monotonically while C_L increases monotonically. However, the total force coefficient D_F decreases at first until it reaches a minimum value around $C = 0.3$, then it starts increasing as the wave-effect parameter C becomes large. At large values of C, the total force is mainly due to its out-of-phase component resulting from surface waves. This can also be shown by figure 7, in which the phase angle θ_F defined by (27*b*) is plotted versus C for several different values of G. We note from figure 7 that θ_F tends to $\frac{1}{2}\pi$ for large values of C regardless of the values of G.

The effect of porosity on the total force is shown in figure 8, in which the total force coefficient D_F is plotted against the wave-effect parameter C for fixed values of the porous-effect parameter G from $G = 0$ to $G = \infty$. It can be seen clearly from figure 8 that, for fixed C, D_F decreases as G increases. When the wavemaker becomes completely 'transparent' to the fluid ($G \to \infty$) the total force on the wavemaker reduces to zero, as it should be, based on physical intuition.

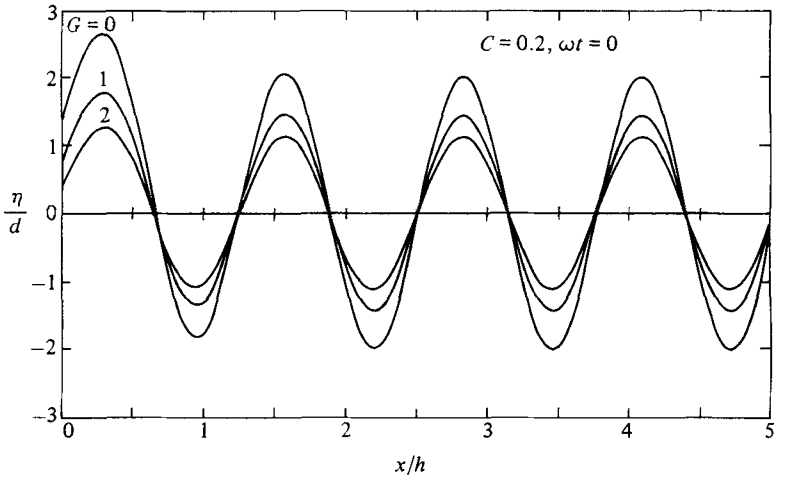

FIGURE 9. Surface-wave profile for different values of G at $C = 0.2$, $\omega t = 0$.

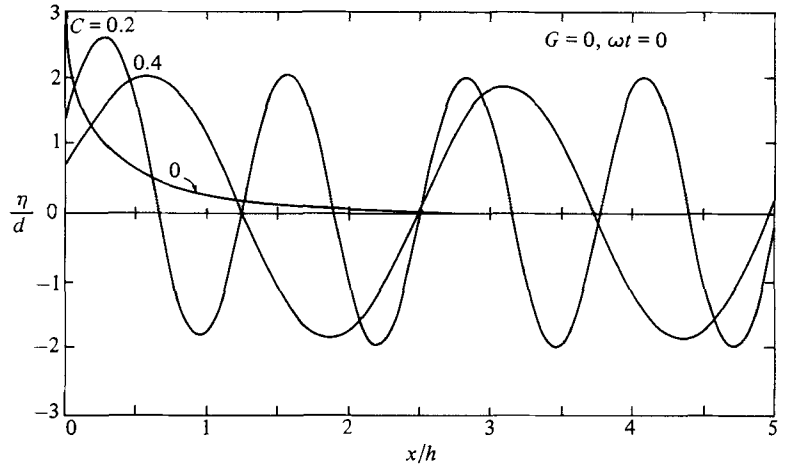

FIGURE 10. Surface-wave profile for different values of C at $G = 0$, $\omega t = 0$.

The free-surface wave profile as calculated by (28) is shown in figure 9 for $C = 0.2$ at $\omega t = 0$. We note from figure 9 that the surface waves produced by an impermeable wavemaker ($G = 0$) have the maximum amplitudes. As G increases, the wave amplitude η/d decreases, since the wavemaker becomes more porous. For a fixed value of G, the first wave has a larger amplitude than those of subsequent waves because of the contribution from non-propagating waves represented by the second term in (28a). As x increases, this contribution decreases exponentially; hence the wave amplitude approaches a constant for given values of C and G. For an impermeable wavemaker, figure 10 shows that, as C increases from 0.2 to 0.4, the wave amplitude decreases slightly while the wavelength almost doubles. In the absence of surface waves ($C = 0$), figure 10 shows that the fluid simply piles up in front of the 'wavemaker' plate.

The important output curve of a porous wavemaker is presented in figure 11, in which the wave amplitude at infinity E_0, as computed from (28b), is plotted against the wave-effect parameter C for various fixed values of the porous-effect parameter

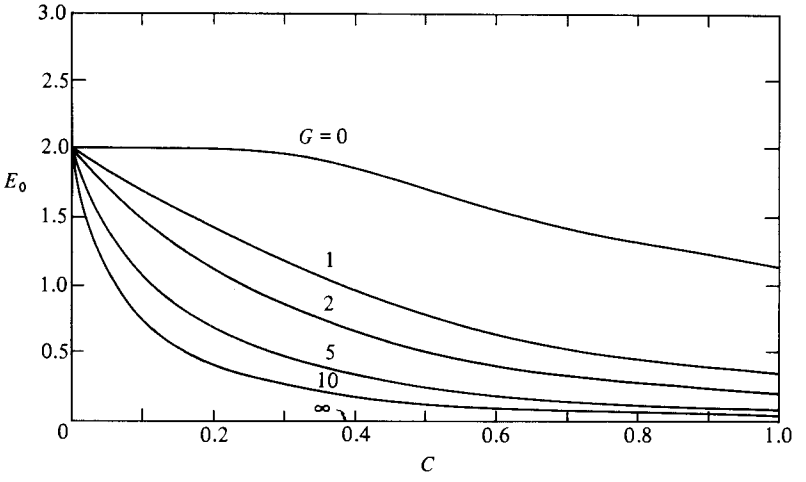

FIGURE 11. Output wave amplitude at infinity versus the wave-effect parameter C for various fixed values of G.

G. We note from figure 11 that, for any fixed values of C, E_0 decreases as G increases. E_0 attains maximum values for an impermeable wavemaker ($G = 0$). On the other hand, E_0 reduces to zero if the wavemaker is completely 'transparent'. For fixed values of G, E_0 decreases as C increases. In the limit as C approaches zero, E_0 tends to a limiting value of 2 for any arbitrary, finite values of G. However, as C becomes very small, the eigenvalue k_0 becomes very large according to (15a); thus the travelling wave at infinity, which is represented by the first term in (28a), has a very short wavelength or oscillates very fast as it should do according to (15c). In the limit when the wave-effect parameter C is identically zero, there will be no surface gravity waves.

I am grateful to Mr L. C. Huang for interesting discussions and for his kind assistance in numerical studies. The author is also very grateful to the referees for their invaluable suggestions. This work was sponsored by the National Science Foundation, under Grant CEE 80-20564 A01.

REFERENCES

BIESEL, F. & SUQUET, F. 1951 Les appareils générateurs de houle en laboratoire. *Houille Blanche* **6**, 147–165, 475–496, 723–737.

CHWANG, A. T. 1978 Hydrodynamic pressures on sloping dams during earthquakes. Part 2. Exact theory. *J. Fluid Mech.* **87**, 343–348.

CHWANG, A. T. 1981 Effect of stratification on hydrodynamic pressures on dams. *J. Engng Maths* **15**, 49–63.

CHWANG, A. T. 1983 Nonlinear hydrodynamic pressure on an accelerating plate. *Phys. Fluids* **26**, 383–387.

HAVELOCK, T. H. 1929 Forced surface-waves on water. *Phil. Mag.* **8**, 569–576.

KENNARD, E. H. 1949 Generation of surface waves by a moving partition. *Q. Appl. Maths* **7**, 303–312.

MADSEN, O. S. 1970 Waves generated by a piston-type wavemaker. In *Proc. 12th Coastal Engng Conf.*, pp. 589–607. ASCE.

NODA, E. 1970 Water waves generated by landslides. *J. Waterways, Harbors & Coastal Engng Div. ASCE* **96**, 835–855.

RAICHLEN, F. & LEE, J. J. 1978 An inclined-plate wave generator. In *Proc. 16th Coastal Engng Conf.*, pp. 388–399. ASCE.

TAYLOR, G. I. 1956 Fluid flow in regions bounded by porous surfaces. *Proc. R. Soc. Lond.* **A234**, 456–475.

URSELL, F., DEAN, R. G. & YU, Y. S. 1960 Forced small-amplitude water waves: a comparison of theory and experiment. *J. Fluid Mech.* **7**, 33–52.

WESTERGAARD, H. M. 1933 Water pressures on dams during earthquakes. *Trans. ASCE* **98**, 418–433.